Load Pull Methodology to Characterize Class-E Outphasing Power Amplifiers

K. Tom   M. Faulkner

Centre for Telecommunications and Micro-Electronics, Victoria University, Australia

E-mail: kevin.tom1@live.vu.edu.au, mike.faulker@vu.edu.au

Abstract—A novel load pull methodology to characterize the performance of class-E outphasing power amplifiers is presented. The traditional analysis of the outphasing topology cannot be applied when class-E amplifiers are used because these amplifiers do not behave as an ideal current or voltage source. Unlike most other amplifier classes, class-E amplifiers require a phase modulated input signal with constant amplitude. Additionally, class-E amplifiers have non-linear transfer characteristics which are a function of the load impedance. The methodology presented here is based on finding the load locus in the load pull plane of an individual class-E amplifier. Then the performance of the two class-E amplifiers in the outphasing topology is readily obtained. The key advantage of the method is that the load pull characterization of only a single amplifier is required. The methodology is general in that any passive load combining circuit can be used and any amplifier combination can be used in the outphasing topology provided that their load pull data is available. The load locus is derived without any reference to the phase difference between the drive signals.

1. INTRODUCTION

There is an increasing demand for highly efficient radio frequency power amplifiers to extend battery/talk time in mobile phones, as well as to reduce the cooling requirements in the base stations. Modern switch-mode radio frequency (RF) power amplifiers (PAs), such as class-E amplifiers, have the potential to achieve very high efficiencies. However, these amplifiers are highly non-linear and they do not behave

1

well with non-constant amplitude signals used by modern wireless systems such as orthogonal frequency division and multiplexing (OFDM) and code-division and multiple-access (CDMA) [1]-[4].

Most amplifier classes achieve their highest efficiency when the amplifier is driven into saturation i.e. at maximum output voltage. The efficiency drops when the output power is backed-off. The outphasing technique introduced by Chireix [5] and the Linear Amplification using Non-linear Components (LINC) introduced by Cox [6] are designed to operate even non-linear amplifiers at saturation, irrespective of the output power. In the outphasing topology the input signal containing both amplitude and phase modulation is separated into two constant envelope phase-modulated signals that are amplified individually and then recombined in a passive power combiner. The benefit is that highly efficient nonlinear PAs, such as class-E amplifiers, can be used to amplify the constant envelope signals without distorting the signal [7]-[10]. Hence, the outphasing topology using class-E amplifiers can be used in modern wireless systems to achieve very high efficiencies.

Outphasing topology commonly employ saturated class-B or class-D amplifiers. In the traditional analysis of outphasing topology the constituent individual amplifiers are assumed to behave like ideal voltage sources [11]. However, this assumption may lead to large discrepancies between simulation and measurements particularly when class-E amplifiers are used. Here we present a methodology to incorporate the non ideal behavior of the constituent amplifiers. Additionally, the methodology can be used to characterize outphasing amplifiers both theoretically and experimentally. We also note that the methodology can be used to characterize outphasing amplifier with any kind of class operation of the constituent amplifiers.

We provide a theoretical analysis of class-E outphasing amplifiers and a detailed explanation for the method to determine its load locus, as originally proposed in [12]. The resulting expression for the load locus on which the individual amplifiers operate is also provided. The load locus is then used to derive the

non-linear transfer function, efficiency, output power, input drive phase and losses associated with the outphasing topology. The load pull methodology is also substantiated by Harmonic Balance analysis.

The proposed load locus method can be used in the design, optimisation and testing of outphasing amplifiers. It enables the designer to predict the outphasing performance from the amplifier load pull data and the combiner network. Performance optimisation is enabled by identifying the regions of the load pull plane that provide optimum performance. The combiner network can then be designed accordingly to bring the load locus to more desirable areas in the load pull plane. Once in production the amplifiers need only be tested in the region of the load locus for stability and performance.

Section II proposes the methodology to determine the operating load locus for outphasing amplifiers. This can then be used along with load pull data of a single amplifier, to derive the operating characteristics of outphasing amplifiers. In Section III the load pull analysis for a single class-E amplifier is provided. Section IV provides the analytical expression for the load locus of class-E amplifiers in the outphasing topology. Finally, in Section V the load locus is used to determine the key amplifier operating properties. The results are presented for both ideal and non-ideal class-E outphasing amplifiers. The results are also compared with an overdriven class-B outphasing amplifier.

2.   METHODOLOGY TO DETERMINE OUTPHASING LOAD LOCUS

Fig. 1a shows the outphasing amplifier topology. Both amplifiers A and B are driven by square pulses with the same amplitude and frequency but with a phase difference $\Delta\phi = \phi_A - \phi_B$. The resultant voltage across the load Z_L is determined by this phase difference. When S_A and S_B are in-phase the voltage difference across Z_L is zero and the current through Z_L is zero, so both amplifiers experience infinite load impedance. When the drive signals are 180^0 out of phase, maximum current flows through Z_L and each amplifier experiences a load of $Z_L/2$. Thus the outphasing causes load modulation. Amplifiers that are ideal voltage sources maintain the same output voltage irrespective of the load impedance; hence the output load voltage is the sum of two constant amplitude phasors as described by the ideal case LINC
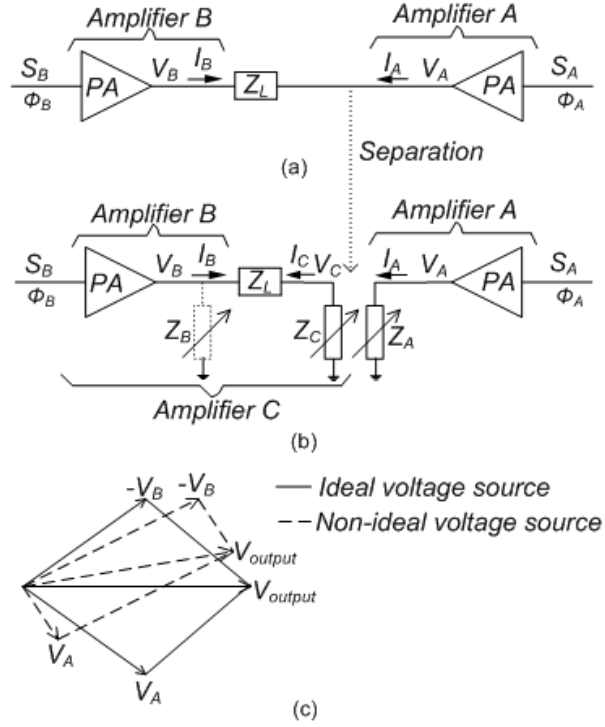
3

Fig. 1. (a) Outphasing topology. (b) Analysis technique using amplifier A and composite amplifier C (c) Ideal amplifier (solid line) and practical amplifier (dashed line).

equations [6]. However, class-E amplifiers do not behave like ideal voltage sources and the output voltage and phase shift through each amplifier are no longer the same as shown in Fig. 1(c). The amplifier that is phase advanced often provides the most power and the resulting output voltage can no longer be predicted by the LINC equations. So the traditional analysis of outphasing amplifiers does not apply to class-E amplifiers. Instead a load pull methodology is proposed as outphasing can be considered as a load modulation technique.

The proposed load pull methodology to characterize outphasing amplifiers is defined in five steps.

1. Determine the load pull data (output voltage contours) of one of the constituent amplifiers in the outphasing topology, say amplifier A in Fig. 2b.

2. Using Z_L, transform the load pull data of the other amplifier, amplifier B in this case, into the load pull data of the composite amplifier C in Fig. 2b.

3. A valid operating point occurs when the impedance and output voltage of both amplifiers A and C are the same i.e. $|V_A| = |V_C|$ and $Z_A = Z_C$.

4. Repeat steps 1-3 to determine the operating point for different voltage and impedance values. The load locus is then obtained by joining the points that satisfy the condition in step 3.

5. Plot the load pull power contours for one of the constituent amplifiers, amplifier A or B. Superimpose the load locus on the load pull power contours to determine the output power of the constituent amplifiers. Other amplifier characteristics like efficiency, losses and drive phase can be obtained similarly.

In this methodology, amplifier B is combined with the load Z_L to form the composite amplifier C as shown in Fig. 1(b). If amplifier A is separated from amplifier C and terminated with a load Z_A, which is adjusted to maintain the same current I_A and voltage V_A, amplifier A will not notice the difference. That is, it will not see any change in its operating condition, since V_A is completely defined by I_A and Z_A as $V_A = Z_A I_A$. Similarly, amplifier C, which includes the load Z_L, sees no change if Z_C is selected such that $I_C = I_A$ and $V_C = V_A$. Please note the different reference directions for I_A, the current *out of* amplifier A, and for I_C, the current *into* amplifier C. If the load pull characteristics of both amplifiers (A and C) are obtained experimentally, then the measured impedance values of one amplifier must be negated to account for the change in direction of the reference current. However, in this analysis the negation is automatically covered by the circuit conventions in the derivation of the $[V_C, Z_C]$ characteristics.

In the load pull analysis of amplifier A, Z_A should cover all values that are expected to be experienced by amplifier A in the outphasing topology. Also the load pull range of amplifier C must cover the same values. At equilibrium, the load pull voltage and impedance must be the same for both amplifiers on either side of the separation. Therefore, the equilibrium conditions are given by

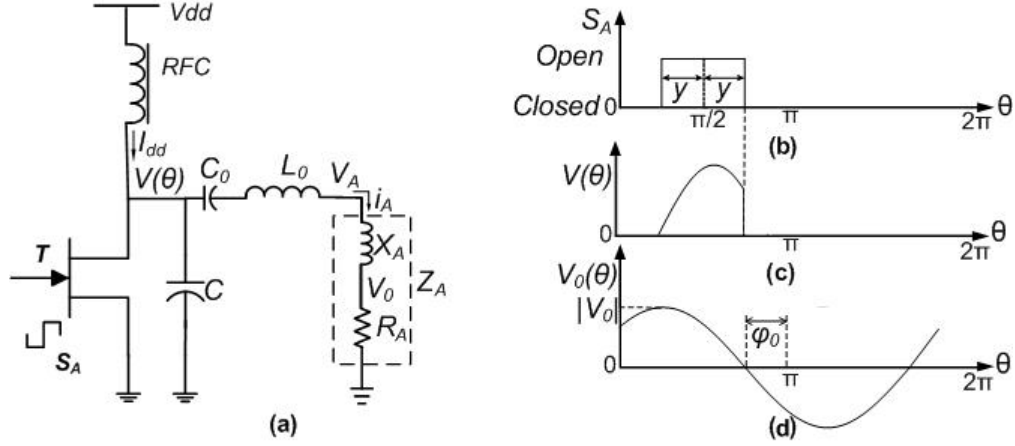$$|V_A| = |V_C| \tag{1}$$

and

$$Z_A = Z_C \tag{2}$$

Fig.2. (a) Class-E Amplifier. (b) Drive signal. (c) Voltage across transistor. (d) Output voltage.

Note that we only need to consider the peak voltage value since both signals have different phase references (S_A for V_A and S_B for V_C). A valid operating point for amplifier A occurs when the $|V_A|$ load pull contour intersects the load pull contours of amplifier C where $|V_A| = |V_C|$ and $Z_A = Z_C$. The operating load locus for each amplifier can then be obtained by determining all intersection points. The load locus describes the amplifier operating point for different outphasing conditions. Note that the analysis technique can work with output power contours as well. The load locus can then be superimposed on the load pull data of single amplifier A to derive the non-linear transfer function, efficiency, output power, input drive phase and losses associated with the outphasing topology. In this analysis with the LINC topology of Fig. 1(a), the load Z_L is a series impedance. However the method also works if shunt admittances are present.

3. LOAD PULL ANALYSIS OF SINGLE CLASS-E AMPLIFIER

To apply the proposed methodology in Section II the load pull data of a single class-E amplifier is required, which can be determined as presented here. The schematic of an ideal Class-E power amplifier is shown in Fig. 2(a). The RF choke (RFC) inductor connects the switching transistor T to the supply voltage Vdd. The transistor contains the parasitic drain to source capacitance, which combines with the external capacitance to form the capacitor C. The series resonant circuit with L_0 and C_0 is tuned to the input signal frequency. The residual reactance X_A ensures a proper phase shift between the output voltage
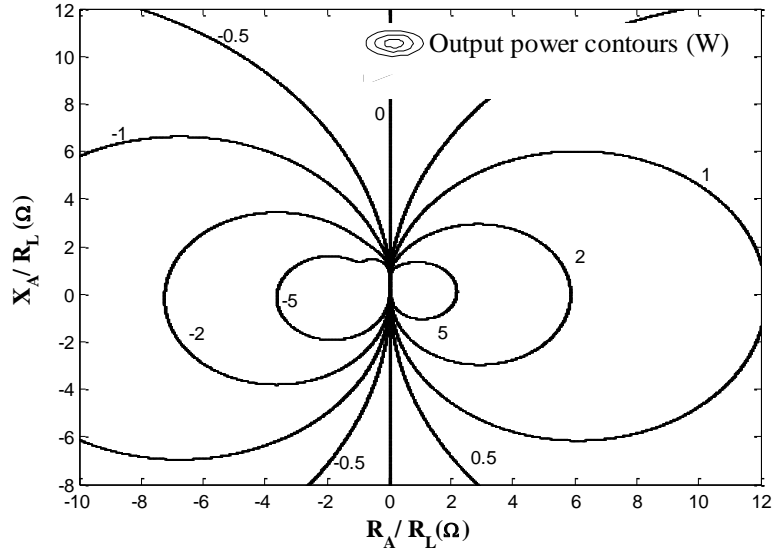
6

Fig. 3. Class-E output power contours as a function of normalised load impedance (normalised to the nominal design load resistance, $R_A = R_L$ (3Ω)).

and drain voltage. The load resistance is R_A. A high efficiency can be achieved by keeping the voltage-current overlap across the transistor as small as possible.

In the analysis presented here, the residual reactance X_A is considered a part of the load network i.e. $Z_A = R_A + jX_A$. Let V_A, be the voltage across Z_A and φ_A, the phase across it. Following Raab's analysis [8] equations for φ_A and V_A can be written as a function of the load Z_A given by

$$\varphi_A = F_0\left(Z_A\right) \tag{3}$$

$$\left|V_A\right| = F_1\left(Z_A\right) \tag{4}$$

where functions F_0, F_1 and its derivations are provided in Appendix (A8) and (A9).

To illustrate the load pull analysis, a Class-E amplifier is analyzed at an operating frequency of 1 GHz using the design equations of [8]. The selected component values are $y = \pi/2$, $C_0 = 0.381$ pF, $L_0 = 66.5$ nH, $V_{dd} = 5.8$ V, $C = 10$ pF, $X_A = X_L = 4.03$ Ω, $R_A = R_L = 3$ Ω, RFC = 40 nH, and $I_{dd} = 0.877$ A. The load

7

pull analysis is performed by varying the load Z_A over the entire range of load values experienced by the outphasing scheme, which will be discussed further in Section IV. The load values must include capacitive values for the residual reactance X_A and negative values for resistance R_A, as for some drive conditions in the outphasing scheme, power flows back into the amplifier. Load pull contours of constant output power, computed from (18) in Appendix versus the normalised class-E load impedance, are plotted in Fig. 3. It is observed that the output power varies from 0 to 5 W for the entire load variation experienced by a single class-E amplifier in an outphasing topology. This load pull analysis of a single class-E amplifier can be applied in an outphasing topology as described in Section IV.

4. LOAD PULL ANALYSIS OF CLASS-E IN OUTPHASING TOPOLOGY

Individual class-E amplifiers in Fig. 2(a) can be combined as in Fig. 1(a) to form the outphasing topology shown in Fig. 4. The residual inductance X_L and the nominal output resistance R_L of each class-E amplifier is considered as part of the outphasing load Z_L indicated by the shaded area in Fig. 4. Let $[V_B, Z_B]$ and $[V_C, Z_C]$ be the voltage and impedance at both ends of the load and I_B, I_C the currents flowing into the load. A unique relationship exists between $[V_B, Z_B]$ and $[V_C, Z_C]$ in terms of the load reactance Z_L. This relationship is obtained by solving for the load network current equations. Thus reactance Z_L transforms the load pull characteristics of amplifier B into the load pull characteristics of the composite amplifier C. In the LINC case the shunt admittances, $+/-jBs$ equal zero, and so the current $I_B = -I_C$ and the solution is given by:

$$V_C = \frac{(Z_B - Z_L)}{Z_B} V_B$$

(5)

$$Z_C = Z_L - Z_B$$

(6)

The above two equations can be used to obtain the load pull contours of amplifier C. First, the load value Z_C is chosen. The load Z_B seen by amplifier B can now be calculated from (6) and then used in Equations
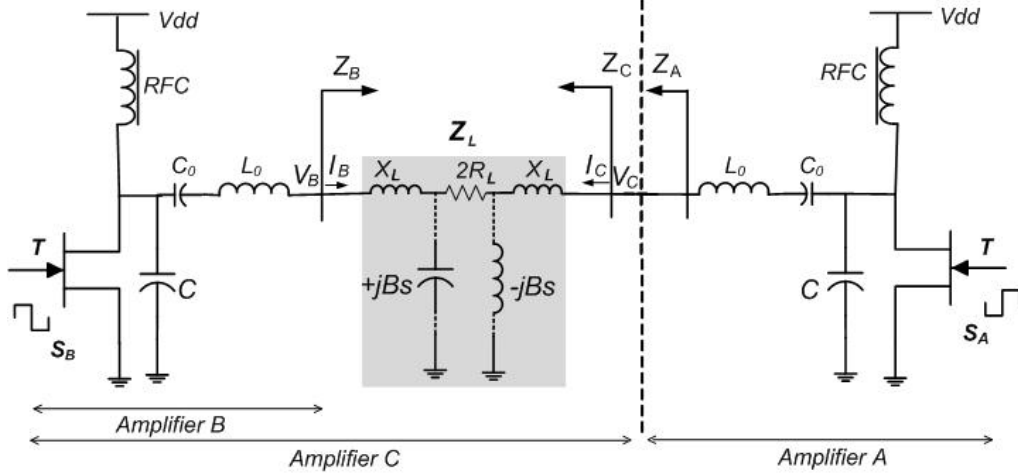
8

Fig. 4. Class-E outphasing /LINC topology. Addition of complimentary shunt reactance $+jBs$ and $-jBs$ (indicated by dotted line) transforms the LINC into a Chireix combiner.

(3) and (4) to calculate φ_B and V_B. Equation (5) enables the calculation of the corresponding values of V_C at the other end of the power combiner. The output voltage of amplifier C as a function of its load is given by

$$|V_C| = \left|\frac{Z_C}{Z_L - Z_C}\right| F_1(Z_L - Z_C)$$

(7)

$$\varphi_C = \angle\left(\frac{Z_C}{Z_L - Z_C}\right) + F_0(Z_L - Z_C)$$

(8)

where φ_C represents the phase shift of V_c with respect to the drive signal S_B, and comprises of the phase shift through the amplifier B and the phase shift attributed to the power combiner network. Following the analysis presented in Section II, a valid operating point for amplifier A occurs when the $|V_A|$ load pull contour intersects the load pull contour of amplifier C where $|V_A| = |V_C|$. Substituting (4) and (7) into (1) and noting (2) provides the characteristic equation for the load locus:

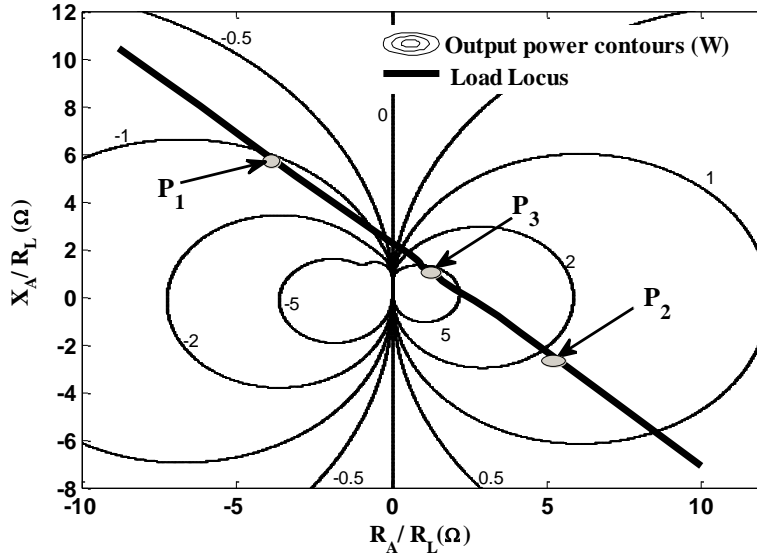$$F_1(Z_A) = \left|\frac{Z_A}{Z_L - Z_A}\right| F_1(Z_L - Z_A)$$

(9)

9

Fig. 5. The load locus for the class-E outphasing topology is superimposed on the Class-E output power contours. Output power is modulated by moving the amplifier operating point up and down the load locus.

The solution of the above equation provides the permissible Z_A values seen by amplifier A in the LINC topology. These load values lie on a trajectory in the load pull plane of amplifier A. The expression for the load locus can be obtained by noting that Z_A is a combination of R_A and X_A and all other parameters are constants. A numerical procedure is used to find the R_A, X_A combinations that satisfy (9).

5.   OUTPHASING LOAD LOCUS ANALYSIS

As an example the load locus is numerically evaluated using the component values of Section III with $Z_L = 2(R_L + jX_L)$, and superimposed on the output power contours of a single class-E amplifier (Fig. 3) as shown in Fig. 5. The output power is modulated along the load locus by the phase difference of the two drive signals. Please note that the analysis technique can work with output power contours as well as peak output voltage contours. Although both amplifiers operate on the same load locus, they do not operate at the same point. If amplifier A sees an impedance Z_A, then from (6) amplifier B sees an impedance of Z_L-Z_A. The load impedance Z_L for the LINC system is the same for both amplifiers and so the operating curve is symmetric around $Z_L/2$. It is almost a straight line when plotted on linear R_A, X_A axes. This is not the

10

case for non-symmetrical circuits, such as non-identical amplifiers or a Chireix combiner, which has a capacitor to ground on one side of the load and an inductor to ground on the other side. In that case the two amplifiers generally work on different load loci.

In Fig. 5 points P_1 and P_2 are the operating points of amplifier A and amplifier B for a specific drive phase of $\Delta\phi = 135^0$. When the drive phases are 180° out of phase each amplifier experiences the same load impedance of $Z_L/2$ (point P_3), which corresponds to optimum class-E operation in this example. When the drives are 315^0 out of phase the amplifiers swap position and points P_1 and P_2 will now be occupied by amplifier B and amplifier A respectively. The total output power is obtained by adding the individual output powers of each amplifier. Additionally, the two points on the load locus can be used to calculate the switching losses for each amplifier and the phase difference of the drive signals. The next paragraph will explain the latter point in more detail.

In this analysis V_A is taken as the reference i.e. $\angle (V_A) = 0$. S_A now has a phase shift of $-\varphi_A$ with respect to V_A. Similarly V_C is made the reference for amplifier C and S_B has a phase shift of $-\varphi_C$ with respect to V_C. The phase difference $\Delta\phi$ between the drives S_A and S_B that is necessary to give the particular valid Z_A value on the load locus is

$$\Delta\phi = (-\varphi_A) - (-\varphi_C) \tag{10}$$

which is evaluated using (3) and (8):

$$\Delta\phi = \angle\left(\frac{Z_A}{Z_L - Z_A}\right) + F_0(Z_L - Z_A) - F_0(Z_A) \tag{11}$$

Fig. 6 shows the output power variation for the two constituent amplifiers across different outphasing angles $\Delta\phi$. It is observed that amplifier B generates more power than amplifier A. For outphasing angles up to 100°, power is flowing back into amplifier A. The reverse power is fully dissipated, as indicated by the amplifier's higher power loss value. At low outphasing angles (0-100°), the output power differs by
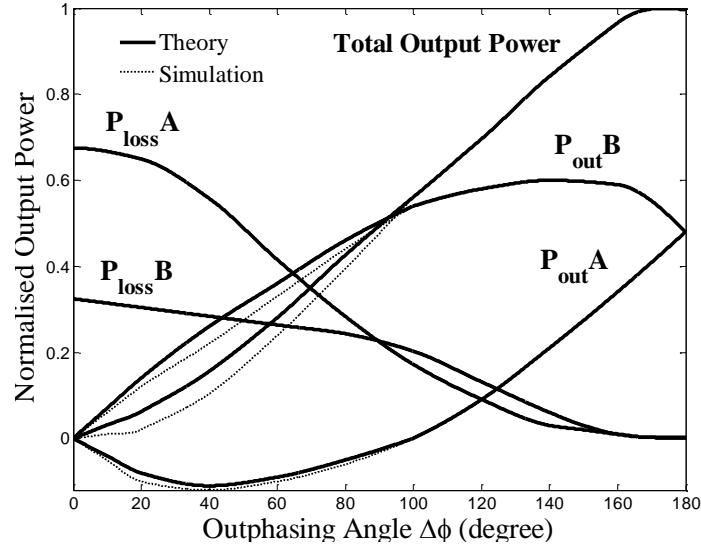
Fig. 6 Class-E LINC output power variation and losses for amplifier A and amplifier B across different outphasing angles. The variation in simulated output power from theory due to second harmonic content can be observed.

up to 2.5% between the theoretical values and those obtained with Agilent's ADS HB simulator. The difference is due to the assumption in the Raab's model of a purely sinusoidal current. In the HB analysis it was observed that the second order harmonic was significant for many drive phases. Increasing the loaded Q of the series tuned network (L_0, C_0) is not effective in suppressing these harmonics. But a wideband harmonic short to ground on either side of the load Z_L proves effective in eliminating the discrepancy, Fig. 7, and theory and HB simulation agree very well.
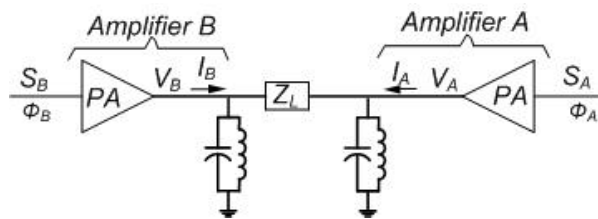

Fig. 7. Class-E outphasing with wideband harmonic short on either side of load Z_L.
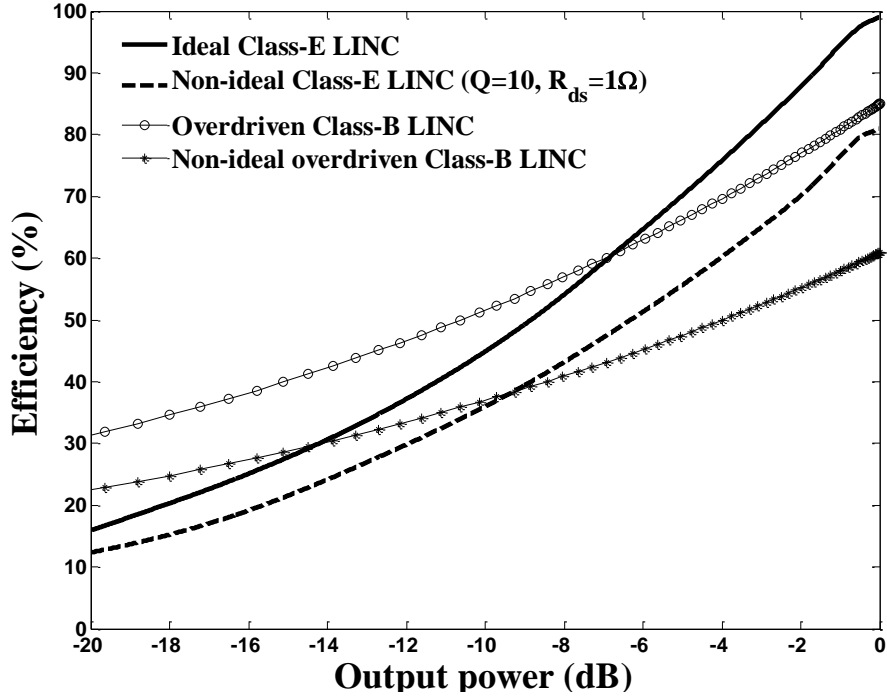
Fig. 8. Outphasing efficiency versus back-off output power.

The efficiency performance of the ideal class-E outphasing amplifier is compared to an overdriven idealized class-B design [3] in Fig. 8. The peak efficiency of the class-E is higher than the class-B but falls more rapidly in back-off. Class-E losses increase quickly as the impedance seen by the amplifier moves away from the optimum load. The class-E outphasing topology is therefore suitable for modulations with approximately less than 7 dB peak to average power ratios. The HB class-E curve includes non-ideal effects of finite Q and R_{ds} resistance. There is a 20% drop in efficiency when these non-ideal effects are included. The Raab model used to derive the load pull curves in this example is a good first order approximation to the generic operation of a class-E amplifier [13]. However, it only includes switching loss, and it is this that limits the accuracy of the efficiency predictions. More inclusive class-E models do exist but they are complicated and non generic [14]-[17], i.e. they only apply to input and load combinations that give optimum class-E operation. Unfortunately, the load pull nature of outphasing amplifiers means that optimum class-E conditions are rare. A generic class-E model that is more accurate than the Raab's model is as yet unavailable.

13

6. CONCLUSION

A method for evaluating the performance of outphasing amplifier with non-ideal component amplifier, i.e. non constant voltage, is presented. To apply the methodology presented in this work, a designer must first determine the load pull data of a single amplifier either through measurement or simulation. Then through Eq. (9) the load locus of the outphasing amplifier is determined. Using this load locus and the load pull data of a single amplifier the characteristics of each of the constituent amplifiers such as efficiency, output power, gain, loss, and drive phase can be determined. This method can be applied to any amplifier combination which uses a passive power combiner provided that their load pull characteristics are available. If this information is to be provided by measurement, active load pull equipment will be necessary to measure the effect of reverse power flow.

The method is used to theoretically derive key performance parameters for the class-E outphasing topology and they are verified by analysis. The proposed methodology is substantiated with rigorous HB analysis which shows a difference of less than 2.5%. The presence of second harmonics in the HB simulations is identified as the root cause of the discrepancy.

7. REFERENCES

[1] www.ericsson.com/technology/whitepapers/sustainableenergy.pdf, accessed July 2011

[2] Larson L., Asbeck P., Kimball D.: 'Next generation power amplifiers for wireless communications - squeezing more bits out of fewer joules', IEEE Radio Frequency integrated Circuits (RFIC) Symposium, Long Beach, CA, USA, June 2005, pp. 417 – 420

[3] Raab F. H., Asbeck P., Cripps S., Kennington P.B., Popovic Z. B., Pothecary N., Sevic J. F., and Sokal N. O.: 'Power Amplifiers and transmitters for RF and microwave', IEEE Trans. Microw. Theory Tech., March 2002, vol. 50, no. 3, pp. 814-826

[4] Cripps S. C. : 'RF Power Amplifiers for Wireless Communication', Norwood: Artech House, 1999.

[5] Chireix H.: 'High power outphasing modulation', Proc. IRE, Nov. 1935, vol. 23, no. 1, pp. 1370-1392.

[6] Cox D. C.: 'Linear amplification with nonlinear components', IEEE Trans. Commun., 1974, vol. 23, no. 1, pp. 1942-1945

[7] Zhang X., Larson L., Asbeck P.: 'Design of Linear RF Outphasing Power Amplifiers', Norwood: Artech House 2003.

[8] Hakala I., Choi D. K., Gharavi L., Kajakine N., Koskela J., Kaunisto R.: 'A 2.14GHz Chireix Outphasing Transmitter', IEEE Tans. Microwave Theory and Techniques, 2005, vol. 53, no. 6, pp. 2129-2138

[9] Wagh P., Midya P. 'High efficiency switched –mode RF powe amplifier'. Proc. 42nd Midwest Symp. On Circuits and Systems, vol. 2, pp. 1044-1047

[10] Bassoo V., Tom K., Mustafa A. K., Cijavet E., Sjoland H., Faulkner M., 'A potential transmitter architecture for future generation green wireless base station', EURASIP J. Wirel. Commun. Netw., 2009, p.8. article id 821846, doi:10.1155/2009/82186

[11] Raab F. H.: 'Idealized Operation of the Class E Tuned Power Amplifier', IEEE Trans. Circuits and Systems, 1977, vol. 24, no. 12, pp. 725-735.

[12] Tom K., Bassoo V., Faulkner M., Lejon T.: 'Load Pull Analysis of Outphasing Class-E Power Amplifier', 2nd IEEE Wireless Broadband and Ultra Wideband Communications-AusWireless, Sydney, Australia, 2007, pp. 52-56.

[13] Raab F. H.: "Effects of Circuit Variations on Class E Tuned Power Amplifier," IEEE journal of Solid State Circuits, 1978, vol. 13, no. 2, pp. 239-247

[14] Kessler D.J., Kazimierczuk M. K.: 'Power losses and efficiency of class-E power amplifier at any duty ratio', IEEE Trans. Circuits and Systems, 2004, vol. 51, no. 9, pp. 1675-1689

[15] Alinikula P.: 'Optimum component values for a lossy class-E power amplifier', IEEE International Microwave Symposium Digest, 2003, vol. 3, pp. 2145-2148

[16] Wang C., Larson L.E., Ashbeck P.M.: 'Improved design technique of a microwave class-E power amplifier with finite switching-on resistance', IEEE Radio and wireless conference (RAWCON), 2002, pp.241-244

[17]   Choi D. K., Long S. I., 'Finite DC feed inductor in class E power amplifiers-a simplified approach', IEEE International Microwave Symposium Digest, 2002, vol. 3, pp. 1643-1646

8.   APPENDIX

Following Raab's analysis [13] (Fig. 2) the design equations are derived under the following assumptions:

1. The inductor RFC is lossless and large enough to neglect its ripple current.

2. The loaded quality factor of the resonant circuit (L_0, C_0) is high enough to ensure that the output current i_A is sinusoidal.

3. The on-resistance of the transistor R_{on} is zero and the transistor turns on and off instantly. The only loss mechanism is the switching loss associated with the instantaneous discharging of the capacitor C on switch closure.

The voltage across R_A is sinusoidal and it can be expressed as $V_0(\theta) = |V_0| \sin(\theta + \varphi_0)$ where $\theta = \omega t$ and ω is the angular switching frequency. $|V_0|$ is the peak value of the output voltage and φ_0 is the phase as defined in Fig. 2(d). The phase reference for the amplifier is set by defining the centre of the input 'off' pulse at $\theta = \pi/2$. Similarly, the expression for the output voltage $V_A(\theta)$ across Z_A, is found as

$$V_A(\theta) = |V_A| \sin(\theta + \varphi_A) \tag{A1}$$

where $|V_A| = |V_0|\sqrt{1 + \left(\dfrac{X_A^2}{R_A^2}\right)} = \rho|V_0|$ and $\rho = \sqrt{1 + \left(\dfrac{X_A^2}{R_A^2}\right)}$.

The phase φ_A across Z_A is given by

$$\varphi_A = \varphi_0 + \psi = \varphi_0 + \tan^{-1}\left(\frac{X_A}{R_A}\right) \tag{A2}$$

16

and represents the phase shift between the voltage, V_A, and the input switching drive signal, S_A. The magnitude of the output voltage across Z_A can be expressed in terms of the circuit parameters given by [8]:

$$|V_A| = I_{dd} R_A \rho g \tag{A3}$$

where I_{dd} is the DC supply current given by

$$I_{dd} = \frac{V_{dd}}{2\pi\omega C}\left(\left(2y^2 + 2yg\sin(\varphi_0 - y)\right) - 2g\sin\varphi_0 \sin y\right) \tag{A4}$$

where g is give by

$$g = \frac{2y\sin(\varphi_A)\sin(y) - 2y\cos(\varphi_A)\cos(y) + 2\cos(\varphi_A)\sin(y)}{-2\sin(\varphi_0 - y)\sin(y)\sin(\varphi_A) - \frac{1}{2}\sin(2y)\cos(2\varphi_0 + \psi) + y\cos\psi} \tag{A5}$$

and φ_0 is given by

$$\varphi_0 = \cot^{-1}\left[\frac{2\pi(1 + \omega C\pi R_A - 2\omega C X_A)}{-8 - 4\omega C\pi R_A + \pi^2(1 - 2\omega C X_A)}\right] \tag{A6}$$

The output power of the class-E amplifier is given by [8]:

$$P_0 = \frac{I_{dd}^2 g^2 R_A}{2} \tag{A7}$$

The above Raab equations are now used to calculate the amplifier's load pull data, which includes output voltage, output power, phase shift through the amplifier and switching losses. For each value of Z_A, the phase angles ψ, φ_A and φ_0 are obtained from (A2) and (A6). The capacitor C, the operating frequency ω, and the switching period y are assumed known. Then I_{dd} and g are calculated using (A4) and (A5) enabling the calculation of $|V_A|$ from (A3). Hence φ_A and $|V_A|$ can be written as

$$F_0(Z_A) = \tan^{-1}\left(\frac{X_A}{R_A}\right) +$$

$$\tan^{-1}\left(\frac{-1 + y^2 - \omega C\pi(R_A + X_A y) + \cos(2y)\sin(y) + y\cos(y)\left[(\omega C\pi R_A) + \sin(y)^2\right]}{(\omega C\pi X_A - y)y\cos(y) + \left(y + \omega C\pi(R_A y - X_A) + y\cos(y)^2\right)\sin(y) - \cos(y)\sin(y)^2}\right) \quad \text{(A8)}$$

$$F_1(Z_A) = I_{dd} R_A \sqrt{1 + \left(\frac{X_A^2}{R_A^2}\right)} \frac{2y\sin(\varphi_A)\sin(y) - 2y\cos(\varphi_A)\cos(y) + 2\cos(\varphi_A)\sin(y)}{-2\sin(\varphi_0 - y)\sin(y)\sin(\varphi_A) - \frac{1}{2}\sin(2y)\cos(2\varphi_0 + \psi) + y\cos\psi} \quad \text{(A9)}$$